Scalable Fluid Models and Simulations for Large-Scale IP Networks

YONG LIU
University of Massachusetts, Amherst
FRANCESCO L. PRESTI
Universita' dell'Aquila
VISHAL MISRA
Columbia University
and
DONALD F. TOWSLEY and YU GU
University of Massachusetts, Amherst

In this article we present a scalable model of a network of Active Queue Management (AQM) routers serving a large population of Transport Control Protocol (TCP) flows. We present efficient solution techniques that allow one to obtain the transient behavior of the average queue lengths and packet loss/mark probabilities of AQM routers, and average end-to-end throughput and latencies of TCP users. We model different versions of TCP as well as different implementations of RED Random Early Detection (RED), the most popular AQM scheme currently in use. Comparisons between the models and ns simulation show our models to be quite accurate while at the same time requiring substantially less time to solve than packet level simulations, especially when workloads and bandwidths are high.

Categories and Subject Descriptors: C.2.6 [**Computer-Communication Networks**]: Internetworking; C.4 [**Performance of Systems**]: *Modeling techniques*

General Terms: Performance

Additional Key Words and Phrases: Fluid model, simulation, large-scale IP networks

This work is supported in part by DARPA under Contract DOD F30602-00-0554 and by NSF under grants EIA-0080119 and ITR-0085848. Any opinions, findings, and conclusions of the authors do not necessarily reflect the views of the National Science Foundation.

Authors' addresses: Y. Liu, Department of Electrical and Computer Engineering, University of Massachusetts at Amherst, 140 Governors Drive, Amherst, MA 01003; email: yongliu@cs.umass.edu; F.L. Presti, Dipartimento di Informatica, Universitá dell' Aquila, Via Vetoio (Coppito 1), 67010 Coppito (AQ), Italy; email: lopresti@di.inivaq.it; V. Misra, Computer Science Department, Columbia University, New York, NY 10025; email: misra@cs.columbia.edu; D. Towsley and Y. Gu, Computer Science Department, University of Massachusetts at Amherst, 140 Governors Drive, Amherst, MA 01003; email: {towsley, yugu}@cs.umass.edu.

1. INTRODUCTION

Networks, and the Internet in particular, have seen an exponential growth over the past several years. The growth is likely to continue for the foreseeable future, and understanding the behavior of this large system is of critical importance. A problem, however, is that the capabilities of simulators fell behind the size of the Internet a few years ago. The gap has since widened, and is growing almost at the same rate as the network is growing. Attempts to close this gap have led to interesting research in the simulation community. It is has been shown computationally expensive to simulate a reasonably sized network. The computation cost grows superlinearly with network size.

In this article, we take recourse to scalable modeling as a tool to speed up "simulations." Our idea is to abstract the behavior of Internet Protocol (IP) networks into analytical models. Solving the models numerically then yields performance metrics that are close to those of the original networks, thereby enabling an understanding of the key aspects of the performance of networks. Our starting point is the model in Misra et al. [2000] that describes the behavior of TCP networks by a set of (coupled) ordinary differential equations. The differential equations represent the expected or mean behavior of the system. Interestingly, recent results [Baccelli et al. 2002; Tinnakornsrisuphap and Makowski 2003] indicate that with appropriate scaling the differential equations in fact represent the *sample path* behavior, rather than the expected behavior. Hence, our solutions gain in accuracy as the size of the network is increased, a somewhat surprising result. We solve the differential equations numerically, using the Runge-Kutta method, and our simulations show speedups of orders of magnitude compared to packet level discrete event simulators such as ns. Additionally, the time-stepped nature of our solution mode lends itself to a particularly simple parallelization. We also perform optimization to identify links that are not bottlenecks to speed up the simulations.

The contribution of this paper goes beyond a numerical implementation of the ideas in Misra et al. [2000]. We address a number of critical deficiencies of the model in Misra et al. [2000]. Most importantly, we incorporate topological information in the set of differential equations. The original model in Misra et al. [2000] defined a traffic matrix, which described the set of routers through which a particular set of flows traversed. However, the *order* in which the flows traversed the routers was ignored in the traffic matrix, and this information is potentially of critical importance. In Section 2.2 we exemplify this with a pathological case wherein the model of Misra et al. [2000] yields misleading results which our refined model corrects. We also model the behavior of a number of variants of TCP such as Selective Acknowledgment (SACK), Reno, and New-Reno in our model. Going beyond the RED [Floyd and Jacobson 1993] AQM mechanism modeled in Misra et al. [2000], we also incorporate other modern AQM mechanisms such as Adaptive Virtual Queue (AVQ) [Kunniyur and Srikant 2001] and Proportional-Integral (PI) control [Hollot et al. 2001].

Two works are particularly relevant to our study. In Bu and Towsley [2001], the authors developed fixed-point solutions to networks similar to ones that we are analyzing, to obtain mean performance metrics. However, that approach suffers from two deficiencies. First, we are often interested in transient behavior of the network, which might reveal potential instabilities. Second, it is not clear from the solution technique outlined in Bu and Towsley [2001] that the solution complexity scales with the size of the network. Another related approach is that of Psounis et al. [2003]. In that approach, the authors exploited the model in Misra et al. [2000] and the ideas of Baccelli et al. [2002] and Tinnakornsrisuphap and Makowski [2003] to demonstrate the fact that the behavior of the network is invariant if the flow population and the link capacities are scaled together. Their approach to simulating large populations of flows over high-capacity links was to scale down the system to a smaller number of flows over smaller-capacity links, thereby making the simulation tractable for discrete event simulators. The idea is appealing (and in fact applies to our approach too); however, the technique only explores the scaling in the population and capacity of the links. Our methodology enables exploring a wider dynamic range of parameters. We can solve larger networks (links and routers) than is possible using discrete event simulators. Preliminary results indicate that the computational requirement of our method grows linearly with the size of the network, whereas the growth of the computational requirement of discrete event simulators is superlinear as the size of the network grows.

We start by deriving the topology-aware fluid model of IP network. The numerical solution algorithm of the fluid model is presented in Section 3. Model refinements are described in Section 4 to account for different versions of TCP and RED implementations. We present some experimental results in Section 5 to demonstrate the accuracy and computational efficiency of our fluid model. Section 6 introduces some extensions to the model. Section 7 concludes the paper and points out directions for future work.

2. FLUID MODELS OF IP NETWORKS

In this section we present a fluid model of a network of routers serving a population of TCP flows. We focus on persistent TCP connections working in the congestion avoidance stage. Models for short-lived TCP flows and timeouts are discussed in Section 6.

2.1 Network Model

We model the network as a directed graph $G = (V, E)$ where V is a set of routers and E is a set of links. Each link $l \in E$ has a capacity of C_l b/s. In addition, associated with each link is an AQM policy, characterized by a probability discarding/marking function $p_l(t)$, which may depend on link state such as queue length. We develop models for AQMs with both marking and dropping. For clarity of presentation, we focus on AQMs with packet dropping unless otherwise explicitly specified. Examples, including RED, will be given in Section 2.4. The queue length of link l is $q_l(t)$, $t \geq 0$. Traffic propagation delay on link l is a_l.

The network G serves a population of N classes of TCP flows. We denote by n_i the number of flows in class i, $i = 1, \ldots, N$. TCP flows within the same class have the same characteristics, follow the same route, and experience the same round-trip propagation delays. Let $F_i = (k_{i,1}, \ldots, k_{i,m'_i})$ and $O_i = (j_{i,n'+1}, \ldots, j_{i,m_i})$ be the ordered set of queues (i.e., links) traversed by the data (forward path) and acks (reverse path) of class i flows, respectively. We distinguish between forward and reverse paths as ack traffic loss is typically negligible compared to data traffic loss. Let $E_i = F_i \cup O_i$. For $k \in E_i$, we let $s_i(k)$ and $b_i(k)$ denote the queues that follow and precede k, respectively.

2.2 The MGT00 Model

In Misra et al. [2000], a dynamic fluid-flow model of TCP behavior was developed using stochastic differential equations. This model relates the expected values of key TCP flows and network variables and is described by the following coupled sets of nonlinear differential equations:

(1) *Window size.* All flows in the same class exhibit the same average behavior. Let $W_i(t)$ denote the expected window size of a class i flow at time t. $W_i(t)$ satisfies

$$\frac{dW_i(t)}{dt} = \frac{1}{R_i(t)} - \frac{W_i(t)}{2}\lambda_i(t), \tag{1}$$

where $R_i(t)$ is the round-trip time and $\lambda_i(t)$ is the loss indication rate experienced by a class i flow. We present expressions for these latter quantities in the next Section. Let $A_i(t)$ denote the (expected) sending rate of a class i flow. This is related to TCP window size by $A_i(t) = W_i(t)/R_i(t)$.

(2) *Queue Length* For each queue l, let N_l denote the set of TCP classes traversing queue l. Then:

$$\frac{dq_l(t)}{dt} = -1(q_l(t) > 0)C_l + \sum_{i \in N_l} n_i A_i(t), \tag{2}$$

where $1(P)$ takes value one if the predicate P is true and zero otherwise.

The first differential equation, (1), describes the TCP window control dynamic. Roughly speaking, the $1/R_i$ term models the window's *additive increase*, while the $W_i/2$ term models the window's multiplicative decrease in response to packet losses, which is assumed to be described by a Poisson process with rate $\lambda_i(t)$.

The second equation, (2), models the average queue length behavior as the accumulated difference between packet arrival rate at the queue, which in Misra et al. [2000] is approximated by term $\sum_{i \in N_l} n_i A_i(t)$, and the link capacity C_l. Observe that the approximation arises in replacing the aggregate arrival rate at the queue at time t with the aggregate sending rate of the TCP flows traversing that queue at t. These two quantities can significantly differ for two reasons: (1) flows are shaped as they traverse bottleneck queues; and (2) the arrival rate at time t at a queue is a function of the sending rate at a time $t - d$, where d is the sum of the propagation and queueing delays from the sender up to the queue. This delay varies from queue to queue and from flow class to flow class. An extreme example consists of one TCP class which traverses two identical RED queues with bandwidth C in tandem. The TCP traffic will be shaped at the first queue so that its peak arrival rate at the second queue is less than or equal

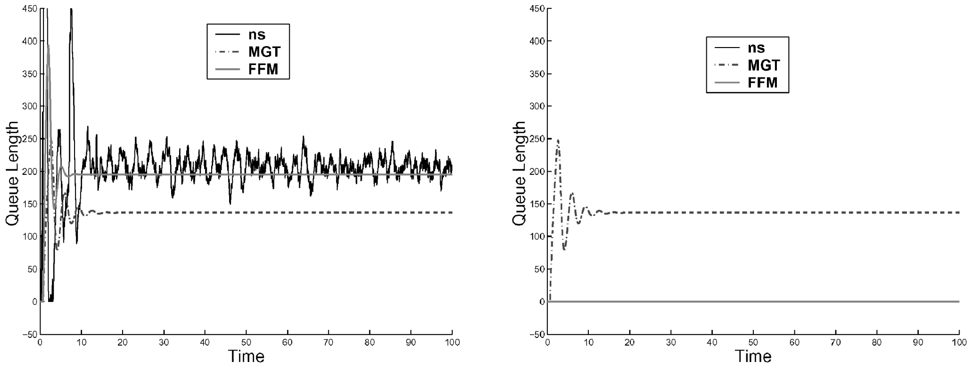

(a) The First Queue

(b) The Second Queue

Fig. 1. Importance of topology order. *ns* = Network Simulator; MGT = Misra-Gong-Towsley; FFM = Fluid-Flow Model.

to C, which equals the service rate of the second queue. Clearly, there won't be any congestion in the second queue. However, from (2), we will get identical equations for those two queues. Therefore the model predicts the same queue length and packet dropping probability for them as shown in Figure 1.

2.3 A Topology Aware Model

We have observed in the previous subsection the importance of accounting for the order in which a TCP flow traverses the links on its path. In this section we present a model that takes into account how flows are shaped and delayed as they traverse the network. This is achieved by explicitly characterizing the arrival and departure rate of each class at each queue. For each queue $l \in F_i$ traversed by class i flows, let $A_i^l(t)$ and $D_i^l(t)$ be the arrival rate and departure rate of a class i flow, respectively. The following expressions relate the departure and arrival process at a queue along the forward path:

—*Departure rate.* When the queue length, $q_l(t)$, is zero, the departure rate at time t equals the arrival rate. When the queue is not empty, the service capacity is divided among the competing flows in proportion to their arrival rates. Thus, for each flow of class i and $l \in F_i$, we have

$$D_i^l(t) = \begin{cases} A_i^l(t), & q_l(t) = 0, \\ \frac{A_i^l(t-d_l)}{\sum_{j \in N_l} A_j^l(t-d_l)} C_l, & q_l(t) > 0, \end{cases} \tag{3}$$

where d_l is the queueing delay experienced by the traffic departing from l at time t. d_l can be obtained as the solution of the following equation:

$$\frac{q_l(t-d_l)}{C_l} = d_l. \tag{4}$$

—*Arrival rate.* For each flow of class i, its arrival rate at the first queue on its route is just its sending rate. On any other queue, its arrival rate is its departure rate from its upstream queue after a time lag consisting of the link propagation delay. It is summarized in the following equation:

$$A_i^l(t) = \begin{cases} A_i(t), & l = k_{i,1}, \\ D_i^{b_i(l)}\left(t - a_{b_i(l)}\right), & \text{otherwise.} \end{cases} \tag{5}$$

The evolution of the system is governed by the following set of differential equations:

(1) *Window size.* The window size $W_i(t)$ of a flow of class i satisfies

$$\frac{dW_i(t)}{dt} = \frac{1(W_i(t) < M_i)}{R_i(t)} - \frac{W_i(t)}{2}\lambda_i(t), \tag{6}$$

where M_i is the maximal TCP window size, and $R_i(t)$ and $\lambda_i(t)$ denote the round-trip time and the loss indication rate at time t (in other words, as seen by the sender at time t). $R_i(t)$ is such that $t - R_i(t)$ is the time at which the data, whose ack has been received at time t, departed the sender. $R_i(t)$ takes the form

$$R_i(t) = \sum_{l \in F_i \cup O_i} a_l + \frac{q_l(t_l)}{C_l}, \tag{7}$$

where t_l is the time at which the data or ack arrived at queue l. $\{t_l, l \in E_i\}$ are related to t by the following set of equations:

$$t_{s_i(l)} = a_l + t_l + \frac{q_l(t_l)}{C_l}, \tag{8}$$

where $t_{k_{i,1}} = t$.

To compute $\lambda_i(t)$ we need to consider the fate of a unit of traffic that departs at time $t - R_i(t)$ at each node along the forward path (assuming ack loss is negligible). The loss indication rate perceived by a TCP class is the summation of lost traffic at all nodes along its path:

$$\lambda_i(t) = \sum_{l \in F_i} A_i^l(t_l) p_l(t_l). \tag{9}$$

(2) *Queue length.* For each queue l, let N_l denote the set of TCP classes traversing it. Then:

$$\frac{dq_l(t)}{dt} = -1(q_l(t) > 0)C_l + \sum_{i \in N_l} n_i A_i^l(t). \tag{10}$$

We repeat the tandem queue experiment in Section 2.2. The revised topology order-aware model gives accurate queue length results at both queues, as shown in Figure 1.

2.4 AQM Policies

The classical AQM policy is RED [Floyd and Jacobson 1993]. RED computes the dropping probability based upon an *average* queue length $x(t)$. The relationship is defined by the following:

$$p(x) = \begin{cases} 0, & 0 \le x < t^{min}, \\ \frac{x - t^{min}}{t^{max} - t^{min}} p^{max}, & t^{min} \le x \le t^{max}, \\ 1, & t^{max} < x, \end{cases} \tag{11}$$

where t^{min}, t^{max}, and p^{max} are configurable parameters. In the $gentle\_$ variant of RED, the following modification is done:

$$p(x) = \begin{cases} 0, & 0 \leq x < t^{min}, \\ \frac{x - t^{min}}{t^{max} - t^{min}} p^{max}, & t^{min} \leq x \leq t^{max}, \\ \frac{x - t^{max}}{t^{max}} (1 - p^{max}) + p^{max}, & t^{max} < x \leq 2t^{max}. \end{cases} \tag{12}$$

In Misra et al. [2000], the differential equation describing $x(t)$ was derived to be

$$\frac{dx}{dt} = \frac{\log_e(1 - \alpha)}{\delta} x(t) - \frac{\log_e(1 - \alpha)}{\delta} q(t), \tag{13}$$

where δ and α are the sampling interval and the weight used in the Exponential Weighted moving Average (EWMA) computation of the average queue length $x(t)$. Thus, the differential equation describing $p_l(t)$ is obtained by appropriately scaling (13) with (11) or (12) according to the scheme used.

We now present the differential equation describing $p_l(t)$ for the PI AQM controller [Hollot et al. 2001]. The PI controller tries to regulate the error signal $e(t)$ between the queue length $q(t)$ and some desired queue length q_{ref} ($e(t) = q(t) - q_{ref}$). In steady state the PI controller drives the error signal to zero. The relationship between $p_l(t)$ and $q(t)$ is described by

$$\frac{dp_l}{dt} = K_1 \frac{dq(t)}{dt} + K_2 \left(q(t) - q_{ref} \right), \tag{14}$$

where K_1 and K_2 are design parameters of the PI algorithm. Note that the REM algorithm [Athuraliya et al. 2001] uses a similar differential equation to compute the *price* at a link, which is subsequently used by a static function to compute the packet dropping probability. Thus, the same scheme used for PI works with a little modification for REM. We have a similar description for AVQ [Kunniyur and Srikant 2001] but do not include it in this article due to space constraints.

2.5 Model Reduction

In most operating networks, congestion only occurs at a small set of links, such as access points and peering points of Internet Service Providers (ISPs). Most network links, especially in backbone networks, operate at low utilization levels. Queues at those links will be always empty and no packet will be dropped. Therefore there is no need to model queueing and RED behavior and maintain TCP states on those links. The network model can be reduced so that we only solve queueing and RED equations for potentially congested links and those *uncongested* links are transparent to all TCP classes except for introducing propagation delays. This can greatly reduce the computation time of the fluid model solver.

Given a network topology and traffic matrix, we can identify *uncongested* links as follows:

—*Step* 1. Define the queue adjacent matrix ADJ such that $ADJ(i, j) = 1$ if there exists a TCP class which traverses queue j immediately after it traverses queue i; $ADJ(i, j) = 0$ otherwise. For queue i, define set $O(i)$ as the set of TCP classes which have queue i as their first hop.

—*Step* 2. Queue i is marked as *uncongested* if

$$\sum_{l \in E} ADJ(l, i) * C_l + \sum_{k \in O(i)} \frac{M_k n_k}{\tau_k} < C_i, \tag{15}$$

where M_k is the maximal TCP window size, n_k is the flow population, and τ_k is two-way propagation delay of TCP class k.

—*Step* 3. Remove all *uncongested* queues from the topology and adjust TCP route accordingly. If all queues on a TCP class's route have been removed, remove this TCP class and calculate its sending rate as $M_k n_k / \tau_k$.

—*Step* 4. If no queue is removed in Step 3, end the model reduction; otherwise, go back to Step 1.

The first term on left-hand side of (15) is the queue i's maximal traffic inflow rate from all its upstream queues. The second term accounts for the fact that a TCP flow's arrival rate at the very first queue on its route is bounded by the ratio of its maximal congestion window to its two way propagation delay.

3. TIME-STEPPED MODEL SOLUTION ALGORITHM

The solution of the fluid model can be obtained by solving the set of delayed differential equations defined in (3)–(14) at a low computational cost. We programmed the fixed step-size Runge-Kutta algorithm [Daniel and Moore 1970] in C to solve the fluid model. The Runge-Kutta algorithm is a widely used method to solve differential equations numerically. Briefly, for a system described by

$$\frac{dy(t)}{dt} = f(t, y(t)),$$

where $y(t) = \{y_1(t), y_2(t), \ldots, y_m(t)\}$, its solution can be obtained by the numerical integration

$$y((n+1)h) = y(nh) + \frac{h}{6}\left[k_{n,1} + 2k_{n,2} + 2k_{n,3} + k_{n,4}\right],$$

where n is the timestep and h is the solution step-size and

$$\begin{aligned}
k_{n,1} &= f\left(t_n, y(nh)\right),\\
k_{n,2} &= f\left(t_n + h/2, y(nh) + k_{n,1}h/2\right),\\
k_{n,3} &= f\left(t_n + h/2, y(nh) + k_{n,2}h/2\right),\\
k_{n,4} &= f\left(t_n + h, y(nh) + k_{n,3}h\right).
\end{aligned}$$

By implementing the Runge-Kutta algorithm, the fluid model solver essentially becomes a time-stepped network simulator. Figure 2 depicts the flowchart of fluid model solver. After reading in network topology and TCP traffic matrix from a configuration file, the fluid model solver conducts model reduction using the algorithm in Section 2.5. Then the fluid model is solved step by step for the whole duration of simulated time. At each time step, the sending rate of each

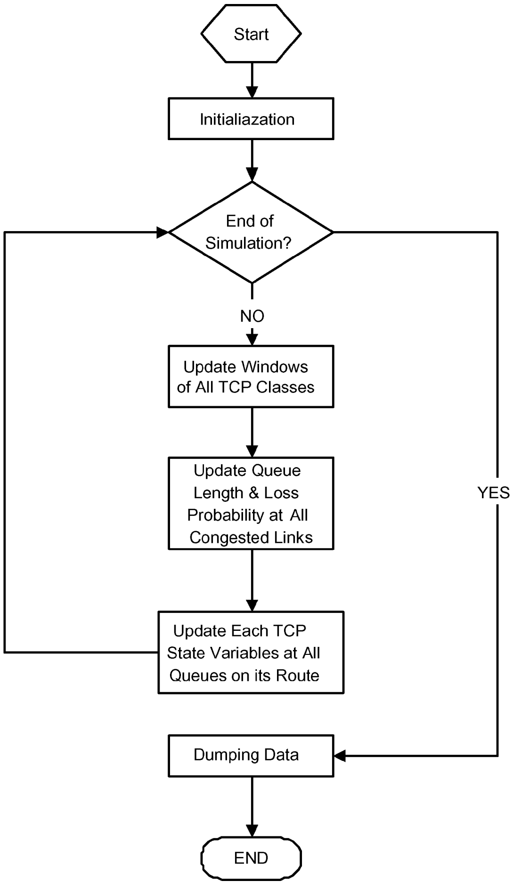
Start
Initialiazation
End of Simulation?
NO
Update Windows of All TCP Classes
Update Queue Length & Loss Probability at All Congested Links
Update Each TCP State Variables at All Queues on its Route
YES
Dumping Data
END

Fig. 2. Flowchart of fluid model solver.

TCP class is updated according to (6); queue lengths and packet loss probabilities at each congested queue are calculated from (10) and the corresponding AQM equations, for example, (11, 12 and 13) for RED; TCP state variables $\{R_i(t), \lambda_i(t), A_i^l(t), D_i^l(t)\}$ are updated according to Equations (3), (5), (7), and (9). The solution of the fluid model, including the sending rate of each TCP class and each congested queue's packet loss probability and queue length, is dumped into data files at the end of the process.

To solve Equations (3), (5), (7), and (9) directly, for each t, we would need to track back in time for each class the instant at which data (ack) arrived at each queue. Instead, we find it convenient to proceed by rewriting those equations *forward* in time, that is, by expressing the future value of the round-trip time, loss rate indication, and arrival and departure rate as functions of their current values. We proceed as follows:

—*Round-trip time.* Let $d_l^i(t)$, $l \in E_i$, $i = 1, \ldots, N$, be the total delay accrued by the unit of data (ack) of flow class i arriving at node l at time t. From the definition,

$$R_i(t) = d^i_{s_i}(t). \tag{16}$$

We compute these delays forward in time as follows:

$$d^i_l\left(t_f\right) = d^i_{b_i(l)}(t) + \frac{q_{b_i(l)}(t)}{C_{b_i(l)}} + a_{b_i(l)}, \tag{17}$$

where $t_f = t + \frac{q_{b_i(l)}(t)}{C_{b_i(l)}} + a_{b_i(l)}$ is the arrival time of a unit of data at link l given that it arrives at the previous link $b_i(l)$ at time t.

—*Loss rate indication.* Let $r^i_l(t), l \in E_i, i = 1, \ldots, N$, be the amount of the flow class i data arriving at link l at time t that is lost. From the definition, we have

$$\begin{aligned}
&\lambda_i(t) = r^i_{s_i}(t), \\
&r^i_l(t_f) = r^i_{b_i(l)}(t) + A^{b_i(l)}_i(t)p_{b_i(l)}(t), && l \in F_i, \\
&r^i_l(t_f) = r^i_{b_i(l)}(t), && l \in O_i.
\end{aligned}$$

—*Departure rate.* The expressions for the departure rate are directly obtained from (3). For each class i and $l \in F_i$,

$$D^l_i\left(t + \frac{q_l(t)}{C_l}\right) = \begin{cases} A^l_i(t), & q_l(t) = 0, \\ \frac{A^l_i(t)}{\sum_{j \in N_l} A^l_j(t)} C_l, & q_l(t) > 0. \end{cases} \tag{18}$$

—*Arrival rate.* For each flow i and $l \in F_i$,

$$A^l_i\left(t + a_{b_i(l)}\right) = D^{b_i(l)}_i(t). \tag{19}$$

The accuracy of the solution of a set of differential equations is determined by the stiffness of the system and the solution step-size. The smaller the step-size, the more accurate the solution. On the other hand, the computation cost to solve differential equations is proportional to the step-size. For our fluid model solver, the tradeoff between step-size and solution accuracy is not stringent. The stiffness of the fluid network model is bounded by the smallest round-trip time of TCP classes and the highest bandwidth of congested queues. We can achieve sufficiently accurate enough results with a small enough step-size. Meanwhile our fluid model solver still runs fast even with a small step-size. As we will see in Section 5, a step-size of 1 ms is small enough for our fluid model solver to get an accurate solution and at the same time enables the solution of a large IP network to be obtained reasonably quickly.

4. REFINEMENTS OF FLUID MODEL

The model in Section 2 captures the basic dynamic behavior of TCP and RED. Real implementations deviate from the basic models in a number of ways. For example, several versions of TCP congestion control, for example, Tahoe, Reno, SACK [Fall and Floyd 1996], have been implemented in different operating systems. In this section, we present some model refinements which account for different versions of TCP and implementations of RED.

4.1 Variants of TCP

Equation (6) models the behavior of TCP Reno. Starting from Reno, TCP implements the *Fast Recovery* mechanism. TCP halves its congestion window whenever the number of duplicate ACKs crosses a threshold. When there are multiple packet losses in a window, TCP Reno reduces its window several times. This makes *Fast Recovery* inefficient. New *Fast Recovery* mechanisms are implemented in Newreno and SACK to ensure at most one window reduction for packet losses within one window. In Fall and Floyd [1996], simulation results showed that Newreno and SACK recover much more quickly than Reno from multiple packet losses.

To model the *Fast Recovery* mechanisms of Newreno and SACK, we replace the perceived packet loss rate $\lambda_i(t)$ in Equation (6) by the following *Effective Loss Rate*:

$$\lambda_i'(t) = \frac{1 - \left(1 - \frac{\lambda_i(t)}{A_i(t-R_i(t))}\right)^{R_i(t)A_i(t-R_i(t))}}{R_i(t)},$$

where $\lambda_i(t)/A_i(t - R_i(t))$ approximates the end-to-end packet loss probability. Consequently, the numerator is the probability that at least one packet is lost within a window of $R_i(t)A_i(t - R_i(t))$ packets. Therefore $\lambda_i'(t)$ models the actual window backoff rate for TCP Newreno and SACK under loss indication rate $\lambda_i(t)$. When the packet loss probability $\lambda_i(t)/A_i(t - R_i(t))$ is small, $\lambda_i'(t) \approx \lambda_i(t)$.

4.2 Compensation for Variance of TCP Windows

Equation (6) yields a stationary value for the average window size, W, of $\sqrt{2/p}$. Other studies [Altman et al. 2000; Padhye et al. 1998] predicted $W = \sqrt{1.5/p}$. We believe that the difference comes from the assumption on loss event process. Our model is a mean-value model: we model only the first-order statistics of TCP window sizes and queue lengths. In a real network, those second-order statistics, for example, variance of TCP window size, impact network stationary behavior. For example, we use the average window size to approximate TCP's window size before backoff. This is accurate if loss arrivals are independent of TCP window size. When the correlation between a TCP class's window size and perceived loss arrival is not negligible, some compensation is necessary. One extreme example is a single bottleneck supporting a single TCP class of M flows. Let W^i denote the window size of ith flow within this class. The average window size of the class is $\bar{W} = \frac{1}{M}\sum_{i=1}^{M} W^i$. Given a small packet loss probability p, the probability that at least one packet in a window will be marked is approximately $W^i p$. Then the average backoff for the whole class is

$$\frac{1}{M}\sum_{i=1}^{M}(W^i)^2 p/2,$$

which is larger than $\bar{W}^2 p/2$. To demonstrate, we conduct an ns simulation of a single-bottleneck network with packet marking. There is only one class of TCP flows. We measure each TCP flow's window size immediately before backoffs. From Figure 3, TCP window sizes before backoffs are generally larger than the

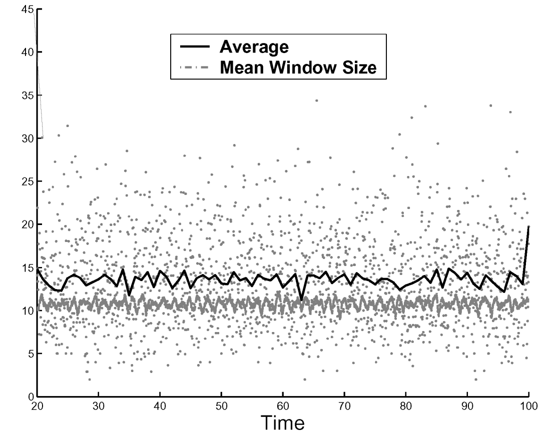

Fig. 3. TCP window sizes prior to backoffs: points plotted are samples of TCP windows over time.

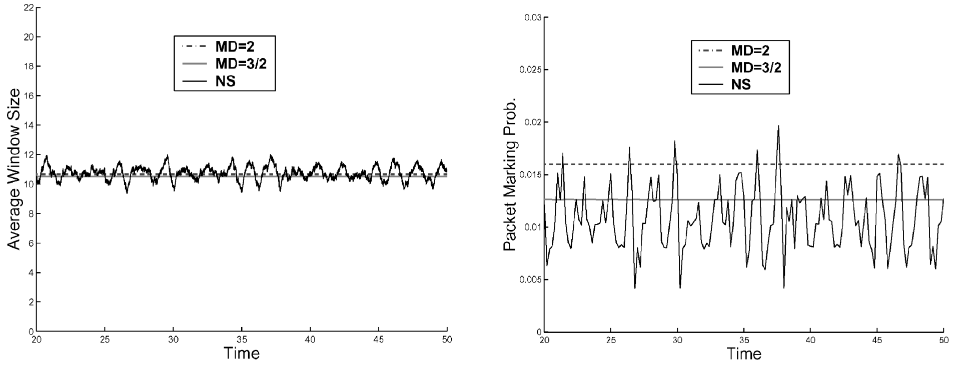

(a) Window Size

(b) Mark Probability

Fig. 4. Compensation for window variance.

average window size. To compensate, we use $\bar{W}/1.5$ instead of $\bar{W}/2$ to model average backoff of a TCP flow. Figure 4 contains results for the ns and fluid models with backoff parameters 1.5 and 2.

4.3 RED Implementation Adjustments

In this section, we model different implementations of RED. Here we assume RED implements packet marking instead of dropping.

—*Geometric and uniform.* After calculating the packet marking probability p based on average queue length, RED marks each packet independently with probability p. Let X be the time interval between two drops. Then X assumes a geometric distribution

$$P(X = k) = (1 - p)^{k-1} p, \quad k = 1, 2, \ldots.$$

In Floyd and Jacobson [1993], the authors pointed out that a geometric intermarking time will cause global synchronization among connections. They then proposed a marking mechanism where X is uniformly distributed in

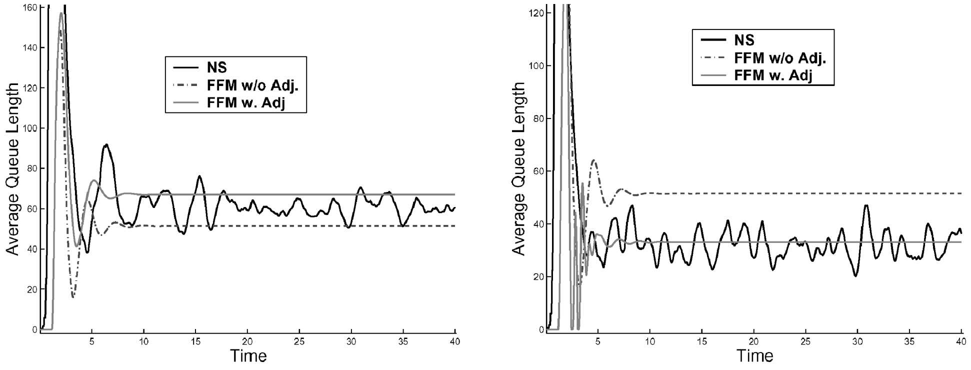

(a) *wait* is on (b) *wait* is off

Fig. 5. Account for RED implementations. NS = Network Simulator; FFM = Fluid-Flow Model.

$[1, 1/p]$. Each arriving packet is marked with probability $p/(1 - count \times p)$, where *count* is the number of packets that have arrived since the last marked packet. A packet will always be marked if $count \times p \geq 1$.

By doing this, the actual packet marking probability is approximately $2p$. To account for uniform marking, the packet marking probability of RED is calculated in the fluid model as

$$p_l(t) = 2 * p\left(x_l(t)\right),$$

where $p(\cdot)$ is the piecewise linear RED marking profile as defined in (12).

—*Wait option.* In the ns implementation, a RED option *wait* is introduced to avoid marking two packets in a row. When *wait* option is on, which is the default for a recent ns version, an arriving packet is marked with probability $p/(2-count \times p)$ if $1 \leq count \times p \leq 2$. A packet will be marked with probability 1 if $count \times p \geq 2$. Intermarking interval X is uniformly distributed in $[1/p, 2/p]$. It effectively reduces the packet marking probability from p to $2p/3$.

To account for those implementation details, we modify the calculation of the RED marking probability in the fluid model to be

$$p_l(t) = \begin{cases} \frac{2}{3}p\left(x_l(t)\right), & wait = 1, \\ 2p\left(x_l(t)\right), & wait = 0. \end{cases}$$

We simulated a single-bottleneck network with a single TCP class of 60 flows. The RED queue at the bottleneck uses Explicit Congestion Notification (ECN) marking. Figure 5 shows the results for the RED queue with and without the *wait* option.

Notice that the packet marking probability predicted by our fluid model is a little higher than the actual packet marking rate in ns. This is because we don't model Timeout. This results in the need for a higher packet marking rate to bring down the TCP sending rates.

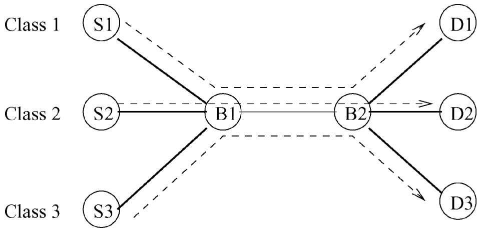

Fig. 6. Single-bottleneck network with dynamic workload.

5. EXPERIMENTAL RESULTS

We have performed extensive experiments to evaluate the accuracy and computation efficiency of our fluid models. We present several representative experiments here. More results are available to interested readers by sending an email request to the authors.

For all the experiments in this section, we use TCP Newreno and RED with ECN marking as the AQM policy. The TCP maximal window size is set to be 128. The step-size of the fluid model solver is fixed at 1 ms. We start with a single-bottleneck topology time-varying TCP workload. The fluid model's accuracy is tested by comparing its solution with simulation results obtained in ns when the network operates in both stable and unstable regions. In Section 5.2, the fluid model's scalability is demonstrated on a two-bottleneck topology. The results show that the fluid model is scalable in the link bandwidth and flow populations. In addition, its accuracy improves as the link bandwidth scales up. In the last experiment, we test the capacity of our fluid model-based simulation on a large topology with more than 1000 nodes and thousands of TCP classes consisting up to 176, 000 TCP flows. Computational results show that the fluid model approach is promising for simulating large IP networks.

5.1 Accuracy of Fluid Model

The first experiment demonstrates the accuracy of our fluid model. As shown in Figure 6, there are three TCP classes. Each TCP class consists of 20 homogeneous TCP flows. The bottleneck link is between B_1 and B_2. It has bandwidth of 10 Mb/s and propagation delay of 25 ms. All other links in the network have bandwidth of 100 Mb/s and propagation delay of 20 ms. There are a total of 14 queues. After model reduction, the fluid model only needs to simulate four queues which potentially have congestion. TCP classes 1 and 2 start at time 0. After 40 s, class 2 stops sending data. The number of TCP flows on the bottleneck link reduces from 40 to 20. The system enters an unstable region. At 70 s, both class 2 and class 3 become active. TCP workload increases by a factor of 3. The system eventually settles around a stable operation point. We compare the fluid model solution with results obtained from ns. Figure 7(a) plots one TCP connection's window sample path and the average window size we obtained from both ns and the fluid model. The fluid model captures the average window behavior very well both when the system is stable and when it is unstable. Figure 7(b) plots the instantaneous queue length from ns and the average queue length predicted by the fluid model. We also observe a good

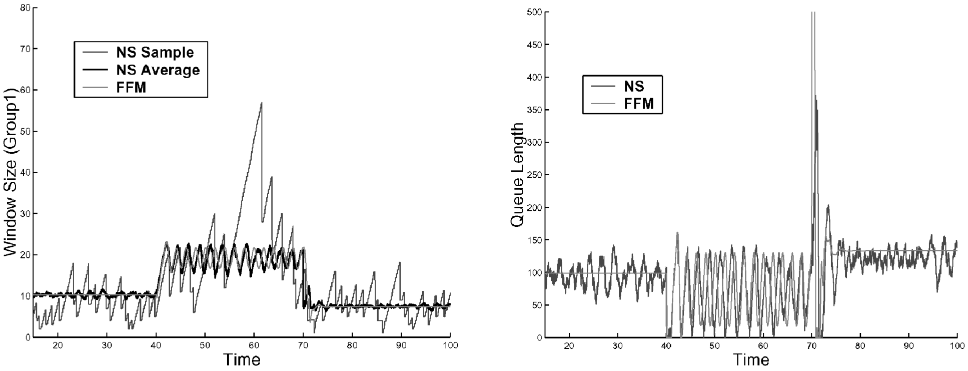

(a) TCP Window Size

(b) Bottleneck Queue

Fig. 7. Results for single-bottleneck topology. NS = Network Simulator; FFM = Fluid-Flow Model.

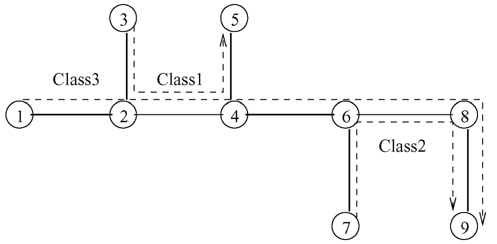

Fig. 8. Network with two bottlenecks.

match, which also implies the fluid model calculates the RED packet marking probability accurately.

5.2 Model Scalability with Link Bandwidth

The second set of experiments demonstrates the fluid model's scalability with link bandwidth and flow populations. We set up three TCP classes on a network of eight links, as in Figure 8.

Link bandwidth and flow population within each class are set to be proportional to a scale parameter K, which ranges from 1 to 100. The link between nodes 2 and 4, and the link between nodes 6 and 8, have bandwidths of $K * 10$ Mb/s. Other links have bandwidths of $K * 100$ Mb/s. Each TCP class consists of $K * 40$ TCP flows. In order for simulation results at different scales to be comparable, we make RED thresholds t^{min} and t^{max} proportional to K and its queue averaging weight α inversely proportional to K. There are a total of 16 queues in the network. Our model reduction algorithm identifies 12 of them as *uncongested* that don't need to be simulated. For each K, we simulate the network for 100 s using both ns and the fluid model solver. Figures 9 and 10 show simulation results for $K = 1$ and $K = 10$, respectively. Tables I and II list simulation statistics of queue lengths and throughputs, including the mean obtained from both ns simulation (ns) and the fluid-flow model (FFM), the standard deviation of ns results,

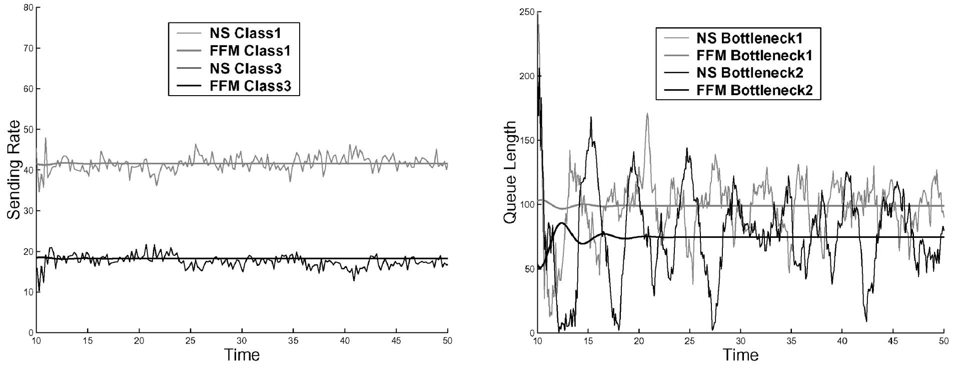

(a) TCP Sending Rate (b) Bottleneck Queues

Fig. 9. Simulation results when $K = 1$. NS=Network Simulator; FFM=Fluid-Flow Model.

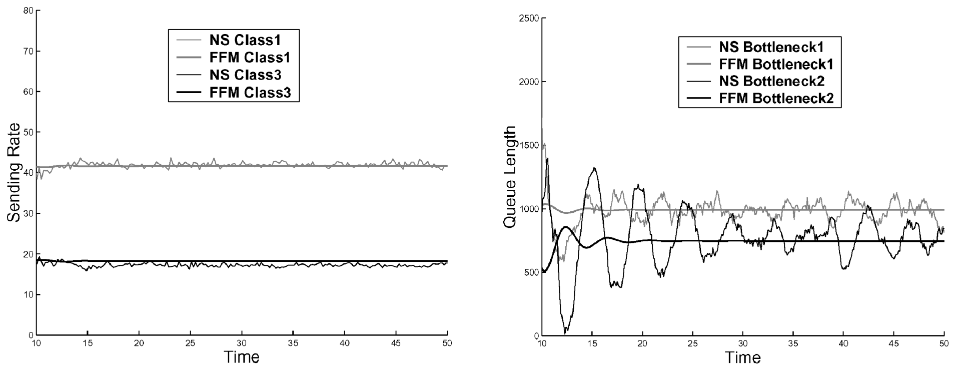

(a) TCP Sending Rate (b) Bottleneck Queues

Fig. 10. Simulation results when $K = 10$. NS=Network Simulator; FFM=Fluid-Flow Model.

and the absolute difference between ns and the fluid model results. ns simulation results eventually converge to the fluid model solution as K gets larger.

Because the fluid model is scalable with both link bandwidth and flow population, the computation cost to obtain model solution is invariant with respect to the scale parameter K. On the other hand, the number of packets that need to be processed in ns grows as link bandwidth and number of flows scale up. It takes much longer for ns simulation to finish when $K = 100$ than when $K = 1$. Table III lists pure computation costs in units of seconds of ns and the fluid model, both without dumping data. The larger the scale, the bigger the computation savings for the fluid model.

5.3 Experience with Large IP Networks

In this experiment, we test our fluid model's capacity to simulate large networks. We use a structured network topology adapted from a baseline network model posed as a challenge to large network simulators by the DARPA Network Modeling and Simulation program.

Table I. Sending Rate of Class 1

K	1	10	50	100
ns mean	42.0	41.6	42.5	41.8
ns Std. dev.	0.59	0.28	0.766	0.21
FFM	41.6	41.6	41.6	41.6
Abs. diff.	1.41	0.47	0.90	0.22

Table II. Queue Length at Bottleneck 1

K	1	10	50	100
ns Mean	100.4	995.4	4875	9942
ns Std. dev.	18.7	59.5	100	162
FFM	99.1	990.5	4953	9905
Abs. diff.	14.5	46.4	91.8	134

Table III. Computation Costs of ns and Fluid Model

K	1	10	50	100
ns	12.5	122	983	1676
FFM	0.766	0.766	0.766	0.766
Speedup	16.32	159.3	1283	2188

At a high level, the topology can be visualized as a ring of N nodes. Each node in the ring represents a campus network and is connected to its two neighbors by links with bandwidth of 9.6 Gb/s and random delays uniformly distributed in the range of 10– 20 ms. In addition, each node is connected to a randomly chosen node other than its neighbors through a chord link. Figure 11(a) illustrates a ring structure generated for $N = 20$.

The campus networks at all nodes share the same topology shown in Figure 11. Each campus network consists of four subnetworks: Net 0, 1, 2, 3. All the links in campus networks have bandwidth of 2.5 Gb/s.

Node 0.0 in Net 0 acts as the border router and connects to border routers of other campus networks. The links within Net 0 have random delays uniformly distributed in the range of 5–10 ms. Links connecting $0.x$ to other subnetworks have random delays uniformly distributed in the range of 1–5 ms. All links in Net 1, Net 2, and Net 3 have random delays of 1–2 ms. Net 1 contains two routers and four application servers. Net 2 and Net 3 each contains four routers connecting to client hosts.

The traffic consists of persistent TCP flows. From each router in Net 2 and Net 3, there are eight TCP classes. Four of them are destined to servers in each router's neighboring campus network. The other four classes are destined to servers in the campus network that connects to the router through a chordal link. Each TCP class contains K homogeneous TCP flows.

In total, the entire network has $19N$ nodes, $44N$ queues, and $64N$ TCP classes. Our experiment is carried on a Dell Precision Workstation 530, which is configured with two Pentium IV processors (2.2 GHz) and 2-GB memory. However, as our program is not parallelized, only one processor is utilized. We fix the flow population of each TCP class at 50 and vary the number of campus networks on the ring from 5 to 55. Each topology is simulated for 100 s.

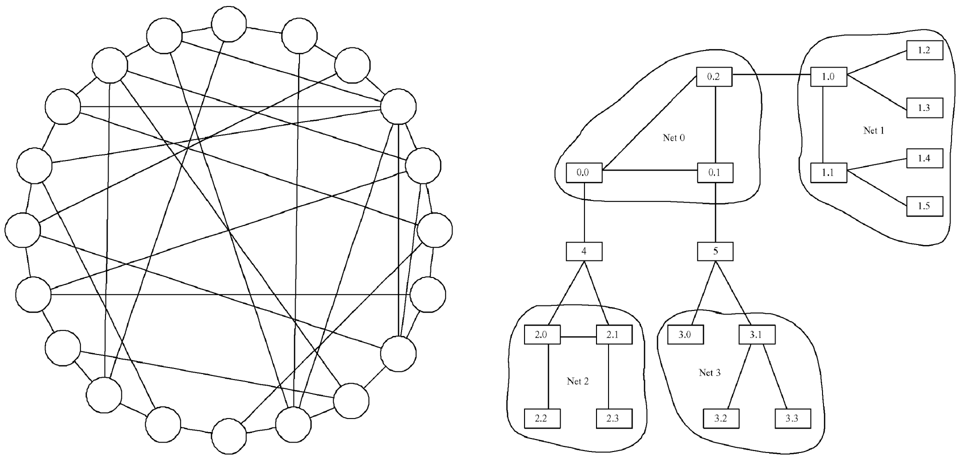

(a) Ring Structure (b) Topology of Subnetworks

Fig. 11. Topology of a large IP network.

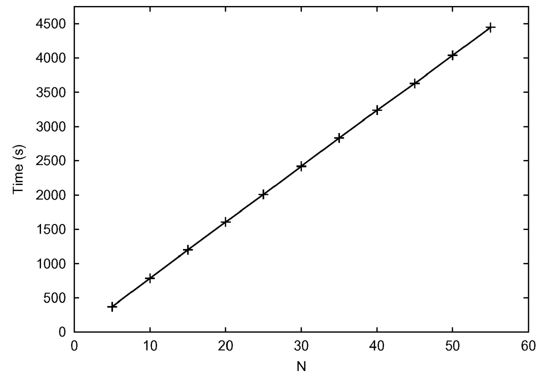

Fig. 12. Computation cost as a function of N.

Our model reduction algorithm identifies nearly 60% queues as *uncongested*. Figure 12 illustrates simulation times that grow almost linearly with the number of campus networks. The simulation of the largest topology, which consists of 1045 nodes and 176, 000 TCP flows, completed after 74 min and 7.2 s when the step-size is set to be 1 ms. This simulation time can be reduced linearly when we use a larger step-size.

6. EXTENSIONS

We have observed in previous sections that our fluid model based approach is promising for simulating large IP networks. In this section, we present some possible model extensions.

6.1 Model Timeout and Slow-Start

The model described in Section 2 captures the Additive Increase Multiplicative Decrease (AIMD) dynamic of the TCP window control. As shown in Misra et al.

[2000], the model can be easily extended to account for timeout losses and the slow-start behavior of TCP, by replacing (6) with

$$\begin{aligned}\frac{dW_i(t)}{dt} &= \left(1-\alpha_{i,CA}\right)\frac{W_i(t)}{R_i(t)} + \alpha_{i,CA}\frac{1}{R_i(t)}\\ &- \frac{W_i(t)}{2}\lambda_i(t)\left(1-p_{i,TO}\right) - \left(W_i(t)-1\right)\lambda_i(t)p_{i,TO}. \qquad (20)\end{aligned}$$

The W_i/R_i term models the exponential growth of the window size in the slow-start phase of TCP, while the $W_i - 1$ term models the window's reduction to 1 in response to timeout losses. $\alpha_{i,CA}$ is the probability that a flow of class i is in congestion avoidance (CA). For long-lived flows, we can ignore the slow-start phase and set $\alpha_{i,CA} = 1$. $p_{i,TO}$ is the probability that a loss is a timeout loss. This probability can be approximated by $p_{i,TO} = \min\{1, 3/W_i\}$ [Padhye et al. 1998].

6.2 Incorporating Unresponsive Traffic

Although the majority of Internet traffic is controlled by TCP, a nonnegligible amount of traffic is unresponsive to congestion. It can be generated by either User Datagram Protocol (UDP) connections or simply TCP connections which are too short to experience congestion. Recent work [Hollot et al. 2003] has studied unresponsive traffic's impacts on AQM performance based on the Misra-Gong-Towsley (MGT) model. We can incorporate unresponsive traffic into our model by changing (10) to

$$\frac{dq_l(t)}{dt} = -1(q_l(t) > 0)C_l + \sum_{i\in N_l} n_i A_i(t) + u_l(t), \qquad (21)$$

where $u_l(t)$ is aggregate unresponsive traffic rate at queue l. Instead of generating individual unresponsive flows, we can use different unresponsive traffic rate models derived in Hollot et al. [2003] for $u_l(t)$ to speed up our simulation.

7. CONCLUSIONS AND FUTURE WORKS

In this article, we have developed a methodology to obtain performance metrics of large, high-bandwidth, IP networks. We started with the basic fluid model developed in Misra et al. [2000], and made considerable improvements and enhancements to it. Most importantly, we made the model developed in Misra et al. [2000] *topology-aware*. That contribution alone is of independent interest in terms of theoretical (fluid) studies of such networks, as topology awareness can play a critical part in conclusions regarding stability and performance, as we demonstrated by a simple tandem queue example. We also incorporated a number of TCP features and variants, as also a number of different AQM schemes into the model. Our solution methodology is computationally extremely efficient, and the scalable model enables us to obtain performance metrics of high-bandwidth networks that are well beyond the capabilities of current discrete event simulators. Our technique also scales well with the size of the network, displaying a linear growth in computational complexity, as opposed to a superlinear growth observed with discrete event simulators. The time-stepped nature of our solution lends itself to a straightforward parallel implementation, pointing to another possible avenue of "simulating" large networks.

As a future work, we will further extend the fluid model and at the same time validate model extensions, including those described in the previous section. The model reduction algorithm described in Section 2.5 still has some space to improve. We are working on integrating our fluid model-based simulator with other existing packet level simulators to conduct *hybrid* simulation. In such a *hybrid* simulation, our fluid simulator can be used to simulate back ground traffic in the core network and provide network delay and loss information to packet traffic running across the fluid core. Preliminary attempts to integrate our fluid simulator with ns have proved successful. Now we are working on parallelizing our fluid simulator to further boost its simulation speed. Some other work that needs to be done is to test the sensitivity of the accuracy of our fluid model in relation to step-size and come up with some guidelines to choose the appropriate step-size. It will be also of interest to compare the solution of the original MGT model and the refined fluid model and identify scenarios where the original model is sufficient to provide a fast solution.

REFERENCES

ALTMAN, E., AVRACHENKOV, K., AND BARAKAT, C. 2000. A stochastic model of TCP/IP with stationary random losses. In *Proceedings of ACM/SIGCOMM '00*.

ATHURALIYA, S., LI, V., LOW, S., AND YIN, Q. 2001. REM: Active queue management. In *IEEE Netw. 15*. 48–53.

BACCELLI, F., MCDONALD, D., AND REYNIER, J. 2002. A mean-field model for multiple TCP connections through a buffer. In *Proceedings of IFIP WG 7.3 Performance*.

BU, T. AND TOWSLEY, D. 2001. Fixed point approximation for TCP behavior in an AQM network. In *Proceedings of ACM/Sigmetrics*.

DANIEL, J. W. AND MOORE, R. E. 1970. *Computation and Theory in Ordinary Differential Equations*. W. H. Freeman, San Francisco, CA.

FALL, K. AND FLOYD, S. 1996. Simulation-based comparisons of Tahoe, Reno, and SACK TCP. *Comput. Comm. Rev. 26*, 3(July), 5–21.

FLOYD, S. AND JACOBSON, V. 1993. Random early detection gateways for congestion avoidance. *IEEE/ACM Trans. Netw. 1,* 4 (Aug.), 397–413.

HOLLOT, C., LIU, Y., MISRA, V., AND TOWSLEY, D. 2003. Unresponsive flows and AQM performance. In *Proceedings of IEEE/INFOCOM*.

HOLLOT, C., MISRA, V., TOWSLEY, D., AND GONG, W. 2001. On designing improved controllers for AQM routers supporting TCP flows. In *Proceedings of IEEE/INFOCOM*.

KUNNIYUR, S. AND SRIKANT, R. 2001. Analysis and design of an adaptive virtual queue algorithm for active queue management. In *Proceedings of ACM/SIGCOMM '2001*.

MISRA, V., GONG, W.-B., AND TOWSLEY, D. 2000. Fluid-based analysis of a network of AQM routers supporting TCP flows with an application to RED. In *Proceedings of ACM/SIGCOMM*.

PADHYE, J., FIROIU, V., TOWSLEY, D., AND KUROSE, J. 1998. Modeling TCP throughput: A simple model and its empirical validation. In *Proceedings of ACM/SIGCOMM '1998*.

PSOUNIS, K., PAN, R., PRABHAKAR, B., AND WISCHIK, D. 2003. The scaling hypothesis: Simplifying the prediction of network performance using scaled-down simulations. *ACM Comput. Comm. Rev. 33*, 1, 35–40.

TINNAKORNSRISUPHAP, P. AND MAKOWSKI, A. 2003. Limit behavior of ECN/RED gateways under a large number of TCP flows . In *Proceedings of IEEE Infocom*.

Received June 2003; accepted November 2003